



**Environmental  
Science**  
Nano

**Emerging investigator series: Differential effects of carbon  
nanotube and graphene on the tomato rhizosphere  
microbiome**

Journal:	<i>Environmental Science: Nano</i>
Manuscript ID	EN-ART-11-2022-001026.R1
Article Type:	Paper

**SCHOLARONE™**  
Manuscripts

### **Environmental Significance**

Carbonaceous nanomaterials (CNMs) can modulate plant development but the underlying mechanism is obscure. Besides influencing pathways in plants, CNMs may impact rhizosphere microbiomes—an essential component of the plant holobiont that contributes to host fitness. This study uses tomato as a model plant to examine how carbon nanotube (CNT) and graphene modulate the rhizosphere microbiome versus the bulk soil microbiome. CNT had a greater impact on the rhizosphere microbiome, significantly shaping its structure and likely its function. Compared to bulk soil microbes, the rhizosphere microbiome had stronger and/or unique responses to CNT. These results will further our understanding of nanomaterial-induced changes in the soil-plant system and contribute to future research on targeted manipulation of rhizosphere microbiomes towards sustainable crop production.

1  
2  
3 **Emerging investigator series: Differential effects of carbon nanotube and graphene on**  
4 **the tomato rhizosphere microbiome**  
5  
6  
7  
8  
9

10 Yaqi You,<sup>1,2,†</sup> Patricia Kerner,<sup>2</sup> Sudha Shanmugam,<sup>3</sup> Mariya V. Khodakovskaya<sup>3</sup>

11  
12  
13  
14 <sup>1</sup>Department of Environmental Resources Engineering, SUNY College of Environmental  
15 Science and Forestry, Syracuse, NY, USA

16  
17 <sup>2</sup>Department of Biological Sciences, Idaho State University, Pocatello, ID, USA

18  
19 <sup>3</sup>Department of Biology, University of Arkansas at Little Rock, Little Rock, AR, USA  
20  
21

22 †Correspondence:

23 Yaqi You

24 402 Baker Lab, 1 Forestry Dr, Syracuse, NY 13210

25  
26 Email: [yyou@esf.edu](mailto:yyou@esf.edu)

27  
28 Phone: +1-315-470-6765  
29  
30  
31  
32  
33  
34  
35  
36  
37  
38  
39  
40  
41  
42  
43  
44  
45  
46  
47  
48  
49  
50  
51  
52  
53  
54  
55  
56  
57  
58  
59  
60

**Abstract**

Application of carbonaceous nanomaterials (CNMs) to the soil-plant system can affect plant physiology, with positive results ranging from enhanced seed germination and root system development to improved stress tolerance. The underlying mechanisms are not fully understood. Plant rhizosphere microbiomes at the soil-root interface are strongly influenced by the host plant and play a key role in the plant host's development and health. Yet few studies have characterized changes in plant rhizosphere microbiomes following applications of CNMs to the soil-plant system. Here we investigated the effects of multi-walled carbon nanotube (CNT) and graphene on microbial communities in the ectorrhizosphere of tomato plants versus surrounding bulk soil. Pot experiments were conducted where tomato plants were exposed to CNT or graphene at 200 mg/kg soil for four weeks. Ectorrhizosphere and bulk soils were then collected and analyzed for physicochemical properties and microbiome structure and function. While graphene had a limited impact on the tomato rhizosphere microbiome, CNT significantly increased microbial alpha diversity, induced greater divergence of beta diversity, enhanced microbial interactions, and potentially impacted community functions such as aromatic compound degradation, antioxidant synthesis, and redox cofactor biosynthesis. Furthermore, CNT induced stronger and/or unique microbiome alterations in the tomato rhizosphere compared to bulk soil. Our findings reveal the differential modulating effects of two widely-used CNMs on plant rhizosphere microbiomes and highlight an imminent need to understand complex plant root-microbe interplays in the CNM-impacted rhizosphere. These results have implication for realizing the full potential of phytoapplication of CNMs toward improved and sustainable plant production.

**Keywords:** nanomaterials, carbon nanotube, graphene, tomato, microbial community, soil microbiome, rhizosphere, metagenomics

## Introduction

The current food and agricultural system faces significant sustainable challenges due to rapid population growth, increasing global food demand and inefficient utilization of resources, and left a huge ecological footprint on the Earth. Nanotechnology is promising to offer innovative solutions to many of these challenges due to its improved capabilities to sense and monitor physical, chemical or biological processes, slowly release fertilizers or nutrients with time, control microbes associated with animal/plant hosts, and mediate biomolecule delivery for genetic engineering of plants.<sup>1-3</sup> Of increasing interest is the phytoapplication of carbonaceous nanomaterials (CNMs).<sup>4-7</sup> They have been shown to enhance seed germination, stimulate plant reproductive systems, increase shoot and root biomass production, activate photosynthesis, boost phytomedicinal contents, and improve plant tolerance and crop yield under salinity and drought stresses.<sup>8-11</sup>

While positive plant phenotypic changes upon CNM application have long been recognized, the underlying mechanisms are not fully understood. Khodakovskaya et al. (2011) reported the uptake of multi-walled carbon nanotubes (CNT) by tomato plants and translocation of CNT to roots, leaves, and fruits, which resulted in the activation of the aquaporin (*LeAqp2*) gene in roots and many stress-signaling genes (e.g., heat shock protein 90 or HSP90 gene) in various tissues, consequently enhancing germination and growth of tomato seedlings.<sup>10</sup> Cao et al. (2020) found that in tomato, multi-walled CNT induced higher nitrate reductase activity and thus endogenous nitric oxide (NO) production, which in turn stimulated lateral root development, likely through NO signaling.<sup>12</sup> Stimulated seed germination and plant growth were observed after the application of not only CNT with different lengths and shapes but also a wide range of other CNMs including graphene and nanohorns.<sup>13,14</sup> Transcriptomics analysis revealed that graphene induced up-regulation of transcriptional factors, plant hormone signal transduction, nitrogen and potassium metabolism, and secondary metabolism in maize roots.<sup>15</sup> More recently, Rezaei Cherati et al. (2021) found that CNT and graphene enhanced tolerance to salinity and drought in tomato, rice, and sorghum by reconciling the expression of affected stress-responsive genes, including those encoding transcription/translation factors, dehydrins, heat shock proteins and aquaporins, and genes involved in calcium transport, mitogen-activated protein kinase (MAPK) signaling cascade, abscisic acid metabolism and signaling.<sup>16</sup> The same study further found that CNT restored more genes than graphene in tomato seedlings under salinity stress, while graphene restored more genes than CNT in rice under drought stress. At the metabolome level, CNT applied to soil as plant growth regulators affected tomato pathways including carbon metabolism, biosynthesis of amino acids and secondary metabolites, amino

1  
2  
3 sugar and nucleotide sugar metabolism, among others.<sup>17</sup> Moreover, foliar-applied carbon dots  
4 were shown to promote maize drought tolerance by increasing the levels of root exudates (e.g.,  
5 succinic acid, pyruvic acid, and betaine).<sup>7</sup>  
6  
7

8 Besides modulating plant biological pathways, CNMs can influence the soil microbiome  
9 through changing microbial abundance, diversity, community composition, and function. To  
10 date, both positive and negative effects of CNMs have been reported, depending on the type of  
11 nanomaterial, the application rate, and the exposure duration.<sup>9,18–20</sup> Soil microbes, especially  
12 those in the rhizosphere, play a key role in the development and health of plant systems.<sup>21–24</sup>  
13 Together they govern nutrient cycling, mediate plant-beneficial functions such as disease  
14 suppression, and form holobionts with the plant hosts.<sup>25</sup> Therefore, many of the CNM-introduced  
15 plant phenotypic changes might result from plant-associated microbiomes. Yet few studies have  
16 elucidated shifts in the rhizosphere microbiome following phytoapplication of CNMs, nor has  
17 research addressed whether the shifts are comparable to those occurring in the bulk soil.  
18  
19

20 This study aimed to bridge this gap by investigating the effects of two widely-used  
21 CNMs, CNT and graphene, on microbial communities in the rhizosphere and surrounding bulk  
22 soil of tomato plants, one of the most consumed vegetable crops around the world. Specifically,  
23 we focused on the ectorrhizosphere, the outermost zone that extends from the rhizoplane next to  
24 the root epidermal cells and mucilage into the bulk soil, because plant-microbe interactions in  
25 this zone strongly influence the host itself.<sup>23,24</sup> We hypothesized that the two CNMs would (1)  
26 modulate the structure and function of tomato-associated microbiomes differentially, and (2)  
27 induce unique microbiome alterations in the tomato rhizosphere that not occur in the bulk soil.  
28 Addressing how various nanomaterials modulate the plant rhizosphere microbiome not only  
29 adds to the understanding of the mechanism underlying nanomaterial-introduced plant  
30 phenotypic changes but may also shed light on harnessing targeted manipulation of the  
31 rhizosphere microbiome using various nanomaterials.  
32  
33  
34  
35  
36  
37  
38  
39  
40  
41  
42  
43

## 44 **Materials and Methods**

### 45 ***Preparation and characterization of CNMs***

46 Surface functionalized (-COOH) multi-walled CNT and graphene nanoplatelets were  
47 purchased from Cheap Tubes (Brattleboro, VT, USA). Multi-walled CNT had an OD of 13–18  
48 nm and a length of 1–12  $\mu\text{m}$ . Graphene had a lateral dimension of 1–2  $\mu\text{m}$  with <3 layers. CNMs  
49 were characterized using transmission electron microscopy (TEM) and Raman spectroscopy as  
50 before.<sup>13,26</sup> CNMs were suspended in sterile MilliQ water and the suspensions were autoclaved  
51  
52  
53  
54  
55  
56  
57  
58  
59  
60

1  
2  
3 three times at 121 °C, 15 lb/in<sup>2</sup> for 20 min to eliminate potential endotoxin contamination as  
4 described by Lahiani et al. (2016).<sup>13</sup>  
5  
6  
7

### 8 ***Plant cultivation and CNM exposure experiments***

9 A model cultivar of tomato (*Solanum lycopersicum* L.), Micro-Tom, was used in this  
10 study. Tomato seeds obtained from Reimer Seeds Co. Inc. (Saint Leonard, MD, USA) were  
11 sterilized as before.<sup>16</sup> Sterile seeds were placed in small germination pots and incubated in a  
12 growth chamber for 21 days with the following conditions: 24 °C, 12 hours of light with a light  
13 intensity of 105 μmol/s m<sup>2</sup>. At the end of the germination period, 3-week-old tomato seedlings  
14 were transferred to experimental pots containing ~400 g of Sun Gro Redi-earth Plug and  
15 Seedling Mix soil (Sun Gro Horticulture, Inc.) for exposure experiments.  
16  
17  
18  
19

20 CNM exposure experiments were conducted in a greenhouse for 3 weeks under the  
21 following conditions: 8-h light (26 C°), 16-h dark (22 C°). In the CNT experiment, six control  
22 plants received 100 mL of deionized water weekly while another 6 plants received 100 mL of  
23 CNT solution (200 μg/mL) weekly for 3 weeks. Similarly, in the graphene experiment, six control  
24 plants received 100 mL of deionized water weekly while another 6 plants received 100 mL of  
25 graphene solution (200 μg/mL) weekly for 3 weeks. The final amount of either CNM in each pot  
26 was approximately 150 mg/kg of soil mix. This concentration was selected because it was  
27 previously found as the most effective nanofertilization concentration for tomato plants.<sup>11</sup> The  
28 selected dose was also comparable to those used in prior studies of CNM effects on the soil-  
29 plant system,<sup>18–20,27–29</sup> although higher than estimated soil concentrations of CNMs.<sup>30,31</sup>  
30  
31  
32  
33  
34  
35  
36  
37

### 38 ***Soil sample collection and processing***

39 Bulk and rhizosphere soils were collected separately from each pot after the exposure  
40 experiment (10 week-old plants), using approaches similar to others.<sup>32,33</sup> First, the tomato plant  
41 was carefully removed from the pot using aseptic technique. Loosely bound soil was removed  
42 from the roots by shaking and using a sterilized spatula. The roots with tightly bound soil (2-5  
43 mm thick) were carefully transferred into a sterile 50 mL centrifuge tube, immediately frozen in  
44 liquid nitrogen, and stored at -80 °C until further processing. For DNA extraction, 15 mL  
45 autoclaved, cold 1X phosphate-buffered saline (pH 7.4) and 15 μL Triton X-100 (0.22 μm  
46 filtered) were added to each 50 mL centrifuge tube containing roots with tightly bound soil. After  
47 gently vortexing, clean roots with minimal soil attached to the surface were carefully removed  
48 from the 50 mL centrifuge tubes using sterilized tweezers. The remaining suspension was  
49  
50  
51  
52  
53  
54  
55  
56  
57  
58  
59  
60

1  
2  
3 centrifuged at 4 °C, 6000x g for 10 min. The resulting supernatant was discarded, and the soil  
4 pellet was used in the DNA extraction as detailed below.

5  
6 For each processed experiment pot, soil in close proximity to the plant's root system was  
7 removed using a sterilized spatula and any small root in the remaining soil was removed with  
8 sterilized tweezers. The remaining bulk soil was then mixed using the sterilized spatula,  
9 transferred into a sterile 50 mL centrifuge tube, immediately frozen in liquid nitrogen, and stored  
10 at -80 °C until DNA extraction. A second set of mixed bulk soil was used in community-level  
11 functional analyses (EcoPlate assay and basal soil respiration test) as detailed below. Additional  
12 mixed bulk soil was archived for soil physicochemical property analyses (details in the SI).  
13  
14  
15  
16  
17  
18

### 19 ***Assessing substrate use pattern and basal respiration of the soil microbial community***

20 Due to the limited amount of rhizosphere soils, only bulk soils were measured for  
21 community-level microbial functionality. Six bulk soils from the CNT experiment (3 control pots  
22 and 3 treatment pots) and eight bulk soils from the graphene experiment (4 control pots and 4  
23 treatment pots) were assessed for substrate use pattern with EcoPlates (Biolog, Hayward,  
24 CA).<sup>34</sup> Each EcoPlate device is a 96-well plate containing a range of substrate sources prepared  
25 in triplicate. Bulk soil was thoroughly mixed, suspended in sterile Milli-Q water (1:10 w/v),  
26 dispersed for 10 min in a FS20 ultrasonic bath (Fisher Scientific, Hampton, NH), and shaken in  
27 an incubator at room temperature, 250 rpm for 20 min. To prevent interference from soil  
28 nutrients while maintaining sufficient inoculant microbes, the soil suspension was diluted by  
29 1:5000, and 150 µL of the diluted suspension was added to each well in an EcoPlate. The plate  
30 was incubated at 25 °C in the dark under a humid condition, and color development was  
31 monitored by measuring optical density at 590 nm ( $OD_{590}$ ) at an interval of approximately 24  
32 hours for ~170 hours using a microplate reader (Synergy HTX, Biotek Instruments, Winooski,  
33 VT). Microbial activity in each microplate, expressed as average well-color development  
34 (AWCD), was determined as follows:  $AWCD = \Sigma(OD_{590,i}/31)$  where  $OD_{590,i}$  is the optical density  
35 value from each well and 31 represents the 31 sole substrate sources in each plate. The final  
36 reading was compared across technical replicates ( $n = 3$ ) and pot replicates ( $n = 3\sim 4$ ). Soil  
37 basal respiration was measured to assess soil microbial activity, using an approach similar to  
38 others.<sup>27</sup> More details about EcoPlate assay and soil respiration measurement are presented in  
39 the SM.  
40  
41  
42  
43  
44  
45  
46  
47  
48  
49  
50  
51  
52  
53  
54  
55  
56  
57  
58  
59  
60

### ***DNA extraction and 16S sequencing***

Total DNA was extracted from bulk (n = 24) and rhizosphere (n = 24) soils using the PowerSoil DNA Kit or the PowerSoil Pro Kit (QIAGEN) following the manufacturer's protocols with minor modifications. Briefly, when the PowerSoil DNA Kit was used, the inhibitor removal step was conducted at 4 °C for 10-20 min. A PowerLyzer homogenizer was used to efficiently grind samples with reduced heat generation. Extracted DNA was further purified using the ethanol precipitation protocol.<sup>35</sup> The quantity and quality of the resulting DNA extractants were evaluated using a NanoDrop 1000 spectrophotometer (Thermo Fisher Scientific) as well as by gel electrophoresis.<sup>36</sup> All the DNA samples were stored at -20 °C before further processing.

Library preparation was conducted similarly to the Earth Microbiome project and as before.<sup>36-38</sup> The V4 region of prokaryotic 16S rRNA gene (~390 bp) was amplified with forward-barcoded 515F primer (5'-3': GTGYCAGCMGCCGCGGTAA) and 806R primer (5'-3': GGACTACNVGGGTWTCTAAT).<sup>39-41</sup> A typical PCR reaction consisted of 20 ng of template DNA in 1 µL, 0.2 µM of each primer, 12 µL of the Invitrogen Platinum Hot Start PCR Master Mix (Thermo Fisher Scientific), and nuclease free water in a total volume of 25 µL. Libraries were cleaned up with the MagBio HighPrep PCR Clean-up System (Illumina), quantified on a CFX96 Touch Real-Time PCR System (Bio-Rad) with the NEBNext Library Quant Kit for Illumina (New England BioLabs), and checked for quality on an 5200 Fragment Analyzer (Agilent Technologies) utilizing the High Sensitivity NGS Fragment Kit (Agilent Technologies). After quantification on a Qubit 4.0 fluorometer (Thermo Fisher Scientific) with the QuantiFluor dsDNA HS System (Promega), the libraries were pooled in equimolar concentrations and sequenced on an Illumina MiSeq platform with the MiSeq Reagent Kit v2 (500-cycles; Illumina). PhiX control v3 was used to ensure a 3-5% spike.

### ***Bioinformatics and statistical analysis***

Paired-end reads (2x250 bp) were subjected to quality control with FastQC (Andrews 2017) and then processed using the QIIME2 pipeline (version 2021.2).<sup>42,43</sup> Briefly, raw reads were trimmed at both ends when mean Phred values dropped below 30 and denoised using DADA2 to resolve amplicon sequence variants (ASVs).<sup>44</sup> This approach allows one to resolve one-nucleotide differences.<sup>45</sup> Rare ASVs (<10 occurrence among all the samples) were filtered out to avoid sequencing errors and artifacts. Prokaryotic taxonomy was assigned using a naive Bayes machine-learning classifier that was trained for the 515F-806R V4 region against the SILVA database (release 138).<sup>46,47</sup> Reads associated with Eukarya, mitochondria and chloroplast, as well as unassigned reads including those without a defined Phylum, were filtered

1  
2  
3 out. The samples from a control pot in the graphene experiment were excluded from further  
4 analysis due to library preparation issues. For comparison purposes, ASVs present in at least 2  
5 samples from the CNT or graphene experiments (68% and 86% reads, respectively) were  
6 retained. This resulted in 146426-336538 reads (median 252095) per sample among all the  
7 soils (n = 46).  
8  
9

10  
11 Community alpha diversity was calculated at the ASV level after rarefaction. Community  
12 beta diversity was analyzed using log transformed ASV abundance and visualized with principal  
13 coordinate analysis (PCoA) of Bray-Curtis and weighted UniFrac distance.<sup>48</sup> Microbial network  
14 analysis was performed using Bray-Curtis distance of agglomerated ASV abundance to the  
15 phylum level (maximum distance set to 0.3). Linear discriminant analysis (LDA) of effect size  
16 (LEfSe) was applied to ASV relative abundance to identify differential taxa that were most likely  
17 to explain differences between samples. For a taxonomy to be considered as discriminative, the  
18 threshold on the absolute value of the logarithmic LDA was set to 2 and the alpha values for the  
19 ANOVA and Wilcoxon tests were set to 0.05.<sup>49</sup>  
20  
21

22 To profile putative microbial functions, we used PICRUST2 (Phylogenetic Investigation of  
23 Communities by Reconstruction of Unobserved States) which expands PICRUST original  
24 database of gene families and reference genomes (>20 fold increase in reference genomes  
25 from the IMG (Integrated Microbial Genomes) database), and is thus more accurate with  
26 reduced bias as rare environmental-specific functions can be more readily predicted.<sup>50</sup> Gene  
27 family abundance was inferred based on Kyoto Encyclopedia of Genes and Genomes (KEGG)  
28 orthologs (KOs) and Enzyme Commission numbers (EC numbers). Pathway abundance was  
29 inferred based on the MetaCyc database through structured mappings of EC gene families. The  
30 nearest-sequenced taxon index (NSTI) was calculated for each input ASV and any ASV with  
31 NSTI > 2 was excluded from the output. Pathway enrichment was identified based on the  
32 PICRUST2 results using DESeq2 and MicrobiomeAnalyst.<sup>51,52</sup>  
33  
34

35 Metagenomic data analysis and visualization were implemented using R (version 4.0.3)  
36 with the package 'tidyverse', 'ggplot2', 'igraph', 'phyloseq', 'phyloseqGraphTest', 'DESeq2',  
37 'vegan', 'ggnetwork', among others.<sup>53-57</sup> Significant differences in alpha and beta diversity were  
38 determined using the nonparametric Kruskal-Wallis test and permutational multivariate analysis  
39 of variance (PERMANOVA), respectively.<sup>58,59</sup> To test the influence of treatment or soil zone on  
40 the microbial network, graph-based permutation test was conducted using the minimum  
41 spanning tree (n = 9999) and the nearest neighbor (NN) tree (knn = 1).<sup>60</sup> If two nodes (phyla)  
42 were of the same treatment condition or soil zone, the edge connecting them was "pure";  
43 otherwise, the edge was "mixed."  
44  
45  
46  
47  
48  
49  
50  
51  
52  
53  
54  
55  
56  
57  
58  
59  
60

### ***Availability of Sequence Data***

All Illumina reads are deposited at the NCBI Sequence Read Archive (SRA), under the BioProject accession number PRJNA900043 (<https://www.ncbi.nlm.nih.gov/bioproject/PRJNA900043>).

## **Results and Discussion**

### ***CNMs changed bulk soil properties***

Variation in soil chemistry, particularly trace metals, could exist among batches of the commercial soil mix used in this study. Still, the inclusion of corresponding controls allowed us to identify changes due to CNM treatment (Table S1). CNT increased bulk soil electrical conductivity (EC) by 74% and SO<sub>4</sub>-S by 250%, while decreasing CaCO<sub>3</sub> by 59% and Fe by 50%. Graphene increased bulk soil CaCO<sub>3</sub> by 52%. Neither nanomaterial influenced soil pH, which remained slightly acid, nor did either CNM affect total N in the soil. These soil physicochemical changes may have resulted directly from the addition of CNMs. CNT was reported to contain higher metal contents than graphene.<sup>61</sup> Both CNMs have high metal adsorption capacity and can immobilize metals in soil.<sup>62</sup> Alternatively, the soil physicochemical changes may be a result of alterations in the soil-plant system (e.g., uptake/release of nutrients by plant, soil enzyme activity). For example, soil amendment with 200 mg/kg CNT was reported to increase corn K uptake and the activity of urease and dehydrogenase in soil, but decreased phosphatase activity.<sup>29</sup> Regardless of the exact mechanism, soil physicochemical property changes could influence the structure and function of the soil microbiome, which in turn affects soil biogeochemistry.

### ***CNT significantly increased microbial diversity in the tomato rhizosphere***

CNT increased microbial richness in bulk soil and the tomato rhizosphere (Figure 1). The average ASVs were 3718 and 3376 for bulk and rhizosphere soils from the control pots, respectively, and 4981 and 4493 ASVs for bulk and rhizosphere soils from the treatment pots, respectively. Similarly, graphene increased microbial richness in bulk soil and the tomato rhizosphere. The average ASVs were 4341 and 3995 for bulk and rhizosphere soils from the control pots, respectively, and 4600 and 4378 for bulk and rhizosphere soils from the treatment pots, respectively. Considering both soil zones, soils from the CNT experiment had a smaller core soil microbiome (27% of all ASVs) than soils from the graphene experiment (51% of all ASVs) (Figure 1).

1  
2  
3 Changes in microbial alpha diversity were further manifested in Shannon index (Figure  
4 2). CNT increased Shannon diversity in both bulk soil and the tomato rhizosphere, with the  
5 increase in the rhizosphere being significant (from 5.92 to 6.33,  $p = 0.037$  in Kruskal-Wallis  
6 test). Consequently, despite the control pots having higher Shannon diversity in bulk soil than  
7 the rhizosphere ( $p = 0.006$ , Kruskal-Wallis test), the CNT treatment pots showed no significant  
8 difference in Shannon diversity between the two soil zones ( $p = 0.200$ , Kruskal-Wallis test). In  
9 the graphene experiment, bulk and rhizosphere soils had no significant difference in microbial  
10 Shannon diversity, and graphene did not affect microbial Shannon diversity in either soil zone.  
11  
12

13  
14  
15  
16 Diversity is one of the most commonly monitored microbial community indices when  
17 studying the influence of CNMs on the soil microbiome, as drastic reduction in microbial  
18 diversity could suggest degraded soil health. Prior research has unveiled mixed effects of  
19 CNMs, depending on the type of nanomaterial, the application rate, and the exposure duration.  
20 One earlier study found that multi-walled CNT had no significant effect on bacterial diversity in  
21 tomato-growing soil.<sup>11</sup> In another study, both single-walled and multi-walled CNT stimulated  
22 bacterial alpha diversity in bulk soil.<sup>18</sup> Fewer studies have investigated the influence of CNMs on  
23 microbial diversity in the rhizosphere. A recent study of *Solanum nigrum* found no significant  
24 effect of multi-walled CNT on the alpha diversity of rhizosphere bacterial or fungal  
25 communities.<sup>20</sup> Here, our results suggest that CNT but not graphene influenced soil  
26 microbiomes substantially, with a greater impact on the tomato rhizosphere than bulk soil. While  
27 these observations could be partially attributed to CNT-introduced soil property changes, a  
28 stronger shift in the rhizosphere suggests that specific conditions in that microenvironment, such  
29 as CNM-induced root exudates, may have contributed to the assembly of a differential  
30 rhizosphere microbiome compared to controls. Indeed, metabolomics analysis revealed that soil  
31 amendment of CNT could induce up- or down-regulation of a variety of pathways in tomato  
32 roots, including carbon metabolism, biosynthesis of amino acids and secondary metabolites,  
33 amino sugar and nucleotide sugar metabolism, among others.<sup>17</sup> Similarly, foliar application of  
34 carbon dots to maize seedlings increased the levels of succinic acid, pyruvic acid, and betaine  
35 in root exudates.<sup>7</sup> It is very likely that in this study, CNMs triggered changes in the tomato root  
36 metabolome. Future multi-omics analyses integrating plant metabolomics and microbial  
37 metagenomics are needed to elucidate mechanisms underlying CNM-induced interplay between  
38 root exudates and the rhizosphere microbiome.  
39  
40  
41  
42  
43  
44  
45  
46  
47  
48  
49  
50  
51  
52  
53  
54  
55  
56  
57  
58  
59  
60

### **CNT induced greater divergence of the tomato rhizosphere microbiome**

The plant rhizosphere microbiome, shaped by plant-microbe coevolution, is known to differ from the bulk soil microbiome.<sup>23</sup> Here we observed distinct microbial communities in bulk soil and the tomato rhizosphere for all the experiment pots ( $p < 0.005$  in PERMANOVA test) (Figure 3). CNT significantly altered microbial beta diversity in both soil zones ( $p < 0.001$  in PERMANOVA test) (Figure 3), such that in the PCoA plot, soils separated from each other by treatment along the primary coordinate (explaining 26% of the total variance) and by soil zone along the secondary coordinate (explaining 14% of the total variance). In contrast, graphene did not affect microbial beta diversity in either soil zone ( $p > 0.1$  in PERMANOVA test) (Figure 3). Instead, soils from the graphene experiment separated primarily by soil zone along the first coordinate, which explains 22% of the total variance. Together, these results reflect that CNT had a much stronger influence than graphene on soil microbial communities.

Studies have reported impacts of CNMs on microbial community structure in bulk soil. Previously, we reported CNT-induced shifts in microbial beta diversity in bulk soils and showed that single-walled CNT typically exerted stronger effects than multi-walled CNT, where application rate and exposure duration were influential factors.<sup>18</sup> In a one-year exposure study, Ge et al. (2016) found that narrow multi-walled CNT (average diameter 7.4 nm) and graphene (average diameter 2.4  $\mu\text{m}$ ) significantly altered soil bacterial communities, whereas wide multi-walled CNT (average diameter  $>13$  nm) did not.<sup>27</sup> Those results were opposite to our observations here, although the multi-walled CNT and graphene used in both studies had comparable dimensions. This discrepancy may reflect the influence of experiment duration (one year versus one month) on the transformation of CNMs in the soil-plant system and the subsequent effects on the soil microbiome.<sup>63</sup>

Foremost, our results suggest that CNT influence was greater than the soil zone itself, whereas graphene did not have such magnificent influence. Similar to us, Ge et al. (2018) reported greater divergence of the soybean rhizosphere microbiome due to CNT compared to graphene, and attributed this phenomenon to the colloidal stability and differing toxicity mechanisms of these two CNMs.<sup>28</sup> A study of the *S. nigrum* rhizosphere, however, found no significant effect of multi-walled CNT on either bacterial or fungal community structure.<sup>20</sup> However, soils used in that study were from highly polluted historical metal mining sites, which may have introduced other confounding factors causing the discrepancy between their and our results. Alternatively, the discrepancy may be owing to rhizosphere conditions specific to the plants used (*S. nigrum* versus tomato). Research of other plant species, especially those of agricultural importance, is warranted to validate the generality of our observations.

### ***CNT affected more taxa in tomato-associated soil microbiomes***

The top 10 bacterial phyla among all the soil samples were Acidobacteriota, Actinobacteriota, Bacteroidota, Chloroflexi, Cyanobacteria, Gemmatimonadota, Myxococcota, Planctomycetota, Proteobacteria and Verrucomicrobiota (Figure 4). As expected, many phyla had differential abundance in bulk soil versus the tomato rhizosphere. Bdellovibrionota, Elusimicrobiota, FCPU426, Fibrobacterota, Myxococcota, Nanoarchaeota, Patescibacteria, SAR324\_clade (Marine\_group\_B), Spirochaetota, Sumerlaeota, and Verrucomicrobiota were enriched in bulk soil, whereas Abditibacteriota, Cyanobacteria, MBNT15, and Proteobacteria were enriched in the tomato rhizosphere ( $p < 0.05$  in Kruskal-Wallis test).

Comparing the two CNMs, CNT significantly affected more prokaryotic taxa than graphene (phylum level results in Figure 4; class level results in Figure S2). In bulk soil, CNT significantly enhanced the phylum Actinobacteriota, Chloroflexi and Sumerlaeota, but suppressed Desulfobacterota, Fibrobacterota, Firmicutes, Spirochaetota and Verrucomicrobiota, whereas graphene significantly enhanced FCPU426, Nitrospirota and Zixibacteria ( $p < 0.05$  in Kruskal-Wallis test). In the tomato rhizosphere, CNT significantly enhanced Actinobacteriota and WS2, but suppressed Cyanobacteria ( $p < 0.05$  in Kruskal-Wallis test), whereas graphene significantly enhanced Abditibacteriota and WPS-2 ( $p < 0.05$  in Kruskal-Wallis test).

Consistent with the taxonomic results above, LEfSe identified a wide range of differential taxa at the phylum or class level that were most likely to explain CNT-introduced microbiome shifts (Figure 5). In general, different taxa in the two soil zones were influenced (Table S2). In bulk soil, CNT enhanced the phylum Latescibacterota and WS2, three classes in the phylum Acidobacteriota, three classes in the phylum Chloroflexi, and one class in each of the phylum Actinobacteriota, Bacteroidota, Elusimicrobiota, Patescibacteria and Verrucomicrobiota. In the rhizosphere, CNT enhanced the phylum WS2, two classes in the phylum Chloroflexi, one class in each of the phylum Acidobacteriota, Actinobacteriota, Armatimonadota, Bacteroidota, Patescibacteria and Proteobacteria. In both bulk soil and the rhizosphere, CNT suppressed the BD2-11 terrestrial group and one class in the phylum Cyanobacteria, Desulfobacterota and Firmicutes. In bulk soil, CNT further suppressed classes in the archaeal phylum Crenarchaeota and in the bacterial phylum Acidobacteriota, Actinobacteriota, Desulfobacterota, Firmicutes, Gemmatimonadota, Patescibacteria, Planctomycetota and Spirochaetota.

Compared to CNT, graphene resulted in only a few differential taxa and these taxa were very different from those observed in the CNT experiment (Figure 5; Table S2). In bulk soil, graphene enriched one class in each of the phylum Armatimonadota, Myxococcota, and

1  
2  
3 Spirochaetota, while inhibiting one class in each of the phylum Cyanobacteria and Nitrospirota.  
4 In the rhizosphere, graphene enriched one class in each of the phylum Abditibacteriota,  
5 Acidobacteriota, Myxococcota and Patescibacteria, and inhibited one class in each of the  
6 phylum Bdellovibrionota, Dadabacteria, Planctomycetota and Sumerlaeota.  
7  
8

9 In general, our results align with prior findings. In a study of the soil-tomato plant system,  
10 multi-walled CNT increased the abundance of Bacteroidota and Firmicutes but decreased  
11 Proteobacteria (particularly Alphaproteobacteria) and Verrucomicrobiota.<sup>11</sup> However, that study  
12 mixed all the soil from the same pot and did not distinguish between rhizosphere and bulk soils.  
13 Another bulk soil study found that single-walled CNT enhanced phyla Bacteroidota and  
14 Proteobacteria but suppressed Actinobacteriota and Chloroflexi, while multi-walled CNT  
15 increased Chloroflexi, the order Bacillales and Clostridiales under the phylum Firmicutes, and  
16 the class Deltaproteobacteria and Gammaproteobacteria under the phylum Proteobacteria.<sup>18</sup> In  
17 one of the few studies of the plant rhizosphere, Chen et al. (2022) observed that multi-walled  
18 CNT increased Actinobacteriota and Chloroflexi but decreased Proteobacteria in the *S. nigrum*  
19 rhizosphere.<sup>20</sup> Our study observed similar CNT-impacted taxa; further, we delineated the  
20 differential effects of CNT on microbial communities in the tomato rhizosphere versus  
21 surrounding bulk soil. Few studies have investigated graphene-induced microbial taxonomic  
22 changes in the plant rhizosphere. Our data indicate a much smaller influence of graphene on  
23 the soil-tomato plant system as compared to CNT. This observation explains the beta diversity  
24 trends reported earlier in this study and is consistent with others.<sup>28</sup> Moreover, CNT suppressed  
25 multiple classes within the phylum Desulfobacterota which are sulfate-respiring bacteria able to  
26 consume end products from aromatic compound breakdown.<sup>64</sup> This may explain substantially  
27 increased  $\text{SO}_4^{2-}$  concentrations in CNT-treated bulk soil, which could in turn influence  
28 extractable metal concentrations (e.g., Cu, Fe, Zn) and thereby EC and CEC (Table S1), as well  
29 as heterogeneous  $\text{CaCO}_3$  nucleation.<sup>65</sup> Previously, applying GeoChip microarray we also  
30 observed inhibition of sulfite reduction by multi-walled CNT but not fullerene.<sup>19</sup> In addition, here  
31 CNT influenced multiple classes in the phylum Acidobacteriota that could decompose natural  
32 polymers.<sup>66</sup>  
33  
34  
35  
36  
37  
38  
39  
40  
41  
42  
43  
44  
45  
46  
47  
48

### 49 ***CNT enhanced microbial interactions in the tomato rhizosphere***

50 Microbial interactions are essential to the structure and function of the soil microbial  
51 community. Here we observed distinct effects of CNT and graphene on microbial networks in  
52 the soil-tomato plant system. In the bulk soil, both CNMs weakened microbial interactions,  
53 illustrated by reduced network edges, particularly shorter-distance edges (Figures 6, S3, and  
54  
55  
56  
57  
58  
59  
60

1  
2  
3 S4). In the tomato rhizosphere, both CNMs likely strengthened microbial interactions, evident by  
4 increased edges (particularly for CNT) and/or shortened edge distance (particularly for  
5 graphene). Graph-based permutation tests further suggest that in the CNT experiment, both  
6 treatment and soil zone were significant factors shaping microbial occurrence network ( $p <$   
7  $0.002$  in NN tree-based permutation test), whereas in the graphene experiment, soil zone but  
8 not treatment was the significant factor shaping microbial network ( $p < 0.001$  and  $p = 0.864$  in  
9 NN tree-based permutation test for soil zone and treatment, respectively) (Figure S5 and S6).  
10  
11  
12  
13

14 The generally disrupting effects of the two CNMs on the bulk soil microbiome are  
15 consistent with their suppression effects on many taxonomic groups in bulk soil as shown in  
16 Figures 4 and 5. In particular, CNT suppressed a large number of microbial taxa than graphene  
17 and thus disturbed the bulk soil microbial network more severely. On the other hand, CNT  
18 significantly increased microbial alpha diversity (Figures 1 and 2) and the abundance of various  
19 microbial taxa (Figures 4 and 5) in the tomato rhizosphere, which may contribute to  
20 strengthened microbial interactions through new microbe-microbe connections. Graphene-  
21 enhanced microbial interactions were mainly due to shorter edge distance, consistent with  
22 graphene's limited influence on microbial alpha diversity and taxonomic shifts in the tomato  
23 rhizosphere. CNM-enhanced microbial integrations in the plant rhizosphere have not been  
24 reported. We speculate that CNMs, particularly CNT, triggered changes in the rhizosphere  
25 metabolome; in response, microbes cooperated to adapt to the CNM-modulated rhizosphere  
26 microenvironment. It should be noted, however, that correlation-based co-occurrence network  
27 does not necessarily predict ecological relationships. We envision that metabolomics analysis,  
28 integrated with metagenomics, will fully address chemical-microbe interplays in CNM-impacted  
29 plant rhizosphere.  
30  
31  
32  
33  
34  
35  
36  
37  
38  
39  
40

#### 41 ***CNT-induced microbial functional changes***

42 Soil microbial communities mediate critical biogeochemical processes and changes in  
43 community structure and/or composition could have a profound influence on soil function. To  
44 address CNM-induced community functional changes, we first performed 16S-based functional  
45 inference. Our results suggest that graphene did not impact microbial functions in either bulk  
46 soil or the tomato rhizosphere. In contrast, CNT affected distinct microbial pathways in bulk soil  
47 and the tomato rhizosphere (Tables S3 and S4). In bulk soil, CNT significantly impacted  
48 nitrogen metabolism ( $p < 0.001$ , FDR  $< 0.005$ ), having negative effects on nitrogen fixation ( $p <$   
49  $0.001$ , FDR =  $0.067$ ) (Tables S3 and S4). This is consistent with a slight decrease in  $\text{NH}_4^+$  after  
50 CNT treatment (Table S1), as well as one of our prior studies where microarray analysis  
51  
52  
53  
54  
55  
56  
57  
58  
59  
60

1  
2  
3 identified suppression of nitrogen fixation, nitrification, dissimilatory nitrogen reduction, and  
4 anaerobic ammonium oxidation in soils treated by multi-walled CNT at 30 or 300 mg/kg of soil.<sup>19</sup>  
5 CNT-induced downregulation of nitrogen metabolism was also seen in a *Pseudomonas*  
6 *aeruginosa* model strain, where 10 mg/L multi-walled CNT induced differential transcriptional  
7 regulation of 2.5 times more genes than graphene at the same concentration.<sup>67</sup>  
8  
9

10  
11 In the rhizosphere, CNT significantly impacted the pathways of aromatic compound  
12 degradation, steroid degradation, phenylalanine metabolism, and methane metabolism,  
13 negatively affecting the modules of benzene degradation, anaerobic toluene degradation, and  
14 tocopherol biosynthesis ( $p < 0.005$ , FDR  $< 0.05$ ) (Tables S3 and S4). Interestingly, CNT  
15 affected F<sub>420</sub> biosynthesis both positively (gene *cofD* and *cofE*) and negatively (gene *cofG* and  
16 *cofH*) (Figure S7). Prior research of CNM impact on the functionality of plant rhizosphere  
17 microbiomes focused on legumes and showed that CNMs may impair symbiotic nitrogen fixation  
18 by inhibiting the initiation of nodulation or symbiosis formation.<sup>28,68</sup> We did not observe  
19 significant impact of either CNT or graphene on microbial nitrogen metabolism in the tomato  
20 rhizosphere, despite of their negative impact on microbial nitrogen fixation in bulk soil. Little is  
21 known about CNM-induced microbial functional shifts in the rhizosphere of non-leguminous  
22 plants. Here the negative effects of CNT on microbial traits might be attributed to the reduced  
23 abundance of the corresponding functional groups. For example, tocopherols (lipophilic  
24 antioxidants within the vitamin-E family) are synthesized exclusively by photosynthetic  
25 organisms, including some cyanobacteria.<sup>69</sup> Our data showed that CNT significantly inhibited  
26 the phylum Cyanobacteria and thus negatively affected tocopherol biosynthesis in the tomato  
27 rhizosphere. The influence of CNT on F<sub>420</sub> biosynthesis has not been reported previously.  
28 Cofactor F<sub>420</sub>, historically known as a methanogenic redox cofactor, is widely distributed across  
29 the bacterial and archaeal domains, catalyzing challenging redox reactions including key steps  
30 in methanogenesis, xenobiotic degradation, and antibiotic biosynthesis. Prokaryotic F<sub>420</sub>  
31 synthesize pathways have three variants, existing in Euryarchaeota (*cofD* and *cofE* present),  
32 Actinobacteriota and Chloroflexi, and Proteobacteria (*cofE* present), but all start with deazaflavin  
33 Fo synthesis mediated by *cofG/H* or *fbfC*.<sup>70</sup> Our data suggest that CNT increased the phylum  
34 Actinobacteriota, the class Alphaproteobacteria and members of Chloroflexi, but decreased the  
35 class Clostridia in the tomato rhizosphere. These groups are known F<sub>420</sub> producers and their  
36 abundance changes might affect F<sub>420</sub> biosynthesis pathways.  
37  
38  
39  
40  
41  
42  
43  
44  
45  
46  
47  
48  
49  
50  
51

52 To further evaluate CNM effects on the functionality of soil microbial communities, we  
53 employed an EcoPlate assay, a culture-dependent analysis of community-level substrate  
54 metabolism. Due to the limited amount of rhizosphere soils, only bulk soils were analyzed. Out  
55  
56  
57  
58  
59  
60

1  
2  
3 of the 31 tested substrates, twenty seven and sixteen substrates were less used in soils treated  
4 by CNT or graphene, respectively, in comparison to control soils (Figure 7). CNT led to less use  
5 of one amine, two amino acids, one carbohydrate, two carboxylic acids and one polymer,  
6 whereas graphene led to less use of one amino acid and one carboxylic acid ( $p < 0.05$  in  
7 Kruskal-Wallis test). Specifically, CNT reduced the microbial use of labile substrates  
8 (amines/amid, amino acids), whereas graphene promoted microbial use of both labile  
9 (amines/amid, amino acids) and complex substrates (polymers). Interestingly, CNT seemed to  
10 promote basal respiration, whereas graphene did not have such an effect (Figure S9). Ge et al.  
11 (2016) also found higher soil basal respiration in CNT-treated soils than controls after one  
12 month of exposure, although over one year, there was no significant difference across  
13 treatments.<sup>27</sup> Our study maintained a higher water content than Ge et al. (2016) (11% versus  
14 5%), which may have contributed to greater soil microbial activities by facilitating the diffusion of  
15 soluble substrates while not limiting the diffusion of oxygen.<sup>71,72</sup> Together, the EcoPlate assay  
16 and basal respiration assessment suggest that the CNT treatment narrowed the substrate  
17 spectrum of microbes but increased their activity in the bulk soil. Whether similar phenomena  
18 also occur in the plant rhizosphere requires further investigation. Specific attention should be  
19 paid to the microbial metabolism of root exudates which are rich in amino acids, organic acids,  
20 sterols, and others.<sup>73</sup>

## 31 32 33 **Conclusion**

34 To realize the full potential of CNMs for sustainable crop production, it is imperative to  
35 elucidate how CNMs influence the plant holobiont which comprises the host plant and its  
36 microbiota. This study depicts the effects of two widely used CNMs, multi-walled CNT and  
37 graphene, on microbiomes in the plant ectorrhizosphere and surrounding bulk soil. We focused  
38 on tomato, one of the most consumed vegetable crops around the world, and identified greater  
39 effects of CNT than graphene on the tomato ectorrhizosphere microbiome. CNT significantly  
40 shaped microbial diversity, community composition, microbe-microbe interaction, and likely also  
41 metabolic activities. Foremost, compared to their counterparts in bulk soil, microbiomes in the  
42 tomato ectorrhizosphere displayed stronger and/or unique shifts in response to CNT, including  
43 greater community divergence, strengthened microbial interaction, and potentially distinct  
44 functional shifts. The significance of these results is twofold. First, it highlights the differential  
45 modulation effects of CNT and graphene on plant rhizosphere microbiomes and the potential  
46 involvement of root exudates that are themselves under CNM modulation. Second, it  
47 emphasizes the need of addressing the influence of rhizosphere microbiome alterations on plant  
48  
49  
50  
51  
52  
53  
54  
55  
56  
57  
58  
59  
60

1  
2  
3 fitness. From a holobiont perspective, root extrudates play an important role in the recruitment  
4 and assembly of the host plant's rhizosphere microbiome, which in turn confers fitness  
5 advantages (e.g., nutrient uptake, stress tolerance, pathogen resistance) to the plant host.  
6 Further research on the interplays between roots and microbes in the CNM-impacted  
7 rhizosphere will help unveil mechanisms underlying CNM-introduced plant phenotypical  
8 changes. It will also shed light on CNM-mediated manipulation of plant rhizosphere  
9 microbiomes for more sustainable crop production.  
10  
11  
12  
13  
14

### 15 **Author contributions**

16 YY and MVK designed the experiments, acquired funding, and supervised the team; SS  
17 and PK conducted the experiments; PK and YY analyzed the data; YY performed bioinformatics  
18 and data curation; YY wrote the original draft; PK and MVK reviewed and edited the manuscript.  
19 All authors have read and agreed to the published version of the manuscript.  
20  
21  
22  
23  
24

### 25 **Conflicts of interest**

26 There are no conflicts of interest to declare.  
27  
28  
29

### 30 **Acknowledgments**

31 Y. You acknowledges support from Idaho State University (the Department of Biological  
32 Science, the College of Science and Engineering) and the State University of New York College  
33 of Environmental Science and Forestry. Y. You also acknowledges Oak Ridge Associated  
34 Universities to sponsor the seminar series "From Genome to Exposome: State of Biosystem  
35 Signaling in Response to Emerging Environmental Stressors" that inspired this research. P.  
36 Kerner was supported by the Center for Ecological Research and Education at Idaho State  
37 University. We thank Dr. Kathleen Lohse (Idaho State University) for providing EGM-4 gas  
38 analyzer, and Lisa McDougall and Jason Werth (Molecular Research Core Facility, Idaho State  
39 University) for completing Illumina sequencing while facing all the challenges associated with  
40 the COVID-19 pandemic. M. Khodakovskaya acknowledges funding from USDA-NIFA (AFRI  
41 2017-07886) and NASA-EPSCoR (NNH16ZHA0055C) which allowed to creation of  
42 infrastructure for experimental work with nanomaterials in UA Little Rock.  
43  
44  
45  
46  
47  
48  
49  
50  
51  
52  
53  
54  
55  
56  
57  
58  
59  
60

## References

1. S. M. Rodrigues, P. Demokritou, N. Dokoozlian, C. O. Hendren, B. Karn, M. S. Mauter, O. A. Sadik, M. Safarpour, J. M. Unrine, J. Viers, P. Welle, J. C. White, M. R. Wiesner and G. V. Lowry, Nanotechnology for sustainable food production: promising opportunities and scientific challenges, *Environ. Sci.: Nano*, 2017, **4**, 767–781.
2. I. O. Adisa, V. L. R. Pullagurala, J. R. Peralta-Videa, C. O. Dimkpa, W. H. Elmer, J. L. Gardea-Torresdey and J. C. White, Recent advances in nano-enabled fertilizers and pesticides: a critical review of mechanisms of action, *Environ. Sci.: Nano*, 2019, **6**, 2002–2030.
3. National Academies of Sciences, Engineering, and Medicine, *Science Breakthroughs to Advance Food and Agricultural Research by 2030*, National Academies Press, Washington, D.C., 2019.
4. A. Gogos, K. Knauer and T. D. Bucheli, Nanomaterials in plant protection and fertilization: current state, foreseen applications, and research priorities, *J. Agric. Food Chem.*, 2012, **60**, 9781–9792.
5. P. Wang, E. Lombi, F.-J. Zhao and P. M. Kopittke, Nanotechnology: a new opportunity in plant sciences, *Trends Plant Sci.*, 2016, **21**, 699–712.
6. T. Hofmann, G. V. Lowry, S. Ghoshal, N. Tufenkji, D. Brambilla, J. R. Dutcher, L. M. Gilbertson, J. P. Giraldo, J. M. Kinsella, M. P. Landry, W. Lovell, R. Naccache, M. Paret, J. A. Pedersen, J. M. Unrine, J. C. White and K. J. Wilkinson, Technology readiness and overcoming barriers to sustainably implement nanotechnology-enabled plant agriculture, *Nat. Food*, 2020, **1**, 416–425.
7. H. Yang, C. Wang, F. Chen, L. Yue, X. Cao, J. Li, X. Zhao, F. Wu, Z. Wang and B. Xing, Foliar carbon dot amendment modulates carbohydrate metabolism, rhizospheric properties and drought tolerance in maize seedling, *Sci. Total Environ.*, 2022, **809**, 151105.
8. S. K. Verma, A. K. Das, S. Gantait, V. Kumar and E. Gurel, Applications of carbon nanomaterials in the plant system: a perspective view on the pros and cons, *Sci. Total Environ.*, 2019, **667**, 485–499.
9. A. Mukherjee, S. Majumdar, A. D. Servin, L. Pagano, O. P. Dhankher and J. C. White, Carbon nanomaterials in agriculture: a critical review, *Front. Plant Sci.*, 2016, **7**, 172.
10. M. V. Khodakovskaya, K. de Silva, D. A. Nedosekin, E. Dervishi, A. S. Biris, E. V. Shashkov, E. I. Galanzha and V. P. Zharov, Complex genetic, photothermal, and photoacoustic analysis of nanoparticle-plant interactions, *Proc. Natl. Acad. Sci. U.S.A.*, 2011, **108**, 1028–1033.
11. M. V. Khodakovskaya, B.-S. Kim, J. N. Kim, M. Alimohammadi, E. Dervishi, T. Mustafa and C. E. Cernigla, Carbon nanotubes as plant growth regulators: effects on tomato growth, reproductive system, and soil microbial community, *Small*, 2013, **9**, 115–123.
12. Z. Cao, H. Zhou, L. Kong, L. Li, R. Wang and W. Shen, A novel mechanism underlying multi-walled carbon nanotube-triggered tomato lateral root formation: the involvement of nitric oxide, *Nanoscale Res. Lett.*, 2020, **15**, 49.

- 1  
2  
3  
4  
5  
6  
7  
8  
9  
10  
11  
12  
13  
14  
15  
16  
17  
18  
19  
20  
21  
22  
23  
24  
25  
26  
27  
28  
29  
30  
31  
32  
33  
34  
35  
36  
37  
38  
39  
40  
41  
42  
43  
44  
45  
46  
47  
48  
49  
50  
51  
52  
53  
54  
55  
56  
57  
58  
59  
60
13. M. H. Lahiani, E. Dervishi, I. Ivanov, J. Chen and M. Khodakovskaya, Comparative study of plant responses to carbon-based nanomaterials with different morphologies, *Nanotechnology*, 2016, **27**, 265102.
  14. M. H. Lahiani, J. Chen, F. Irin, A. A. Poretzky, M. J. Green and M. V. Khodakovskaya, Interaction of carbon nanohorns with plants: uptake and biological effects, *Carbon*, 2015, **81**, 607–619.
  15. Z. Chen, J. Zhao, J. Song, S. Han, Y. Du, Y. Qiao, Z. Liu, J. Qiao, W. Li, J. Li, H. Wang, B. Xing and Q. Pan, Influence of graphene on the multiple metabolic pathways of Zea mays roots based on transcriptome analysis, *PLoS ONE*, 2021, **16**, e0244856.
  16. S. Rezaei Cherati, S. Shanmugam, K. Pandey and M. V. Khodakovskaya, Whole-transcriptome responses to environmental stresses in agricultural crops treated with carbon-based nanomaterials, *ACS Appl. Bio. Mater.*, 2021, **4**, 4292–4301.
  17. S. Rezaei Cherati, M. Anas, S. Liu, S. Shanmugam, K. Pandey, S. Angtuaco, R. Shelton, A. N. Khalfoui, S. V. Alena, E. Porter, T. Fite, H. Cao, M. J. Green, A. G. Basnakian and M. V. Khodakovskaya, Comprehensive Risk Assessment of Carbon Nanotubes Used for Agricultural Applications, *ACS Nano*, 2022, **16**, 12061–12072.
  18. F. Wu, Y. You, X. Zhang, H. Zhang, W. Chen, Y. Yang, D. Werner, S. Tao and X. Wang, Effects of various carbon nanotubes on soil bacterial community composition and structure, *Environ. Sci. Technol.*, 2019, **53**, 5707–5716.
  19. F. Wu, Y. You, D. Werner, S. Jiao, J. Hu, X. Zhang, Y. Wan, J. Liu, Bin Wang and X. Wang, Carbon nanomaterials affect carbon cycle-related functions of the soil microbial community and the coupling of nutrient cycles, *J. Hazard. Mater.*, 2020, **390**, 122144.
  20. X. Chen, J. Wang, Y. You, R. Wang, S. Chu, Y. Chi, K. Hayat, N. Hui, X. Liu, D. Zhang and P. Zhou, When nanoparticle and microbes meet: The effect of multi-walled carbon nanotubes on microbial community and nutrient cycling in hyperaccumulator system, *J. Hazard. Mater.*, 2022, **423**, 126947.
  21. A. H. Ahkami, R. Allen White, P. P. Handakumbura and C. Jansson, Rhizosphere engineering: enhancing sustainable plant ecosystem productivity, *Rhizosphere*, 2017, **3**, 233–243.
  22. M.-J. Kwak, H. G. Kong, K. Choi, S.-K. Kwon, J. Y. Song, J. Lee, P. A. Lee, S. Y. Choi, M. Seo, H. J. Lee, E. J. Jung, H. Park, N. Roy, H. Kim, M. M. Lee, E. M. Rubin, S.-W. Lee and J. F. Kim, Rhizosphere microbiome structure alters to enable wilt resistance in tomato, *Nat. Biotechnol.*, 2018, **36**, 1100–1109.
  23. P. Trivedi, J. E. Leach, S. G. Tringe, T. Sa and B. K. Singh, Plant–microbiome interactions: from community assembly to plant health, *Nat. Rev. Microbiol.*, 2020, **18**, 607–621.

- 1  
2  
3 24. Q. Qu, Z. Zhang, W. J. G. M. Peijnenburg, W. Liu, T. Lu, B. Hu, J. Chen, J. Chen, Z. Lin and  
4 H. Qian, Rhizosphere microbiome assembly and its impact on plant growth, *J. Agric. Food*  
5 *Chem.*, 2020, **68**, 5024–5038.  
6  
7 25. P. Vandenkoornhuysse, A. Quaiser, M. Duhamel, A. Le Van and A. Dufresne, The  
8 importance of the microbiome of the plant holobiont, *New Phytol.*, 2015, **206**, 1196–1206.  
9  
10 26. Y. You, K. K. Das, H. Guo, C.-W. Chang, M. Navas-Moreno, J. W. Chan, P. Verburg, S. R.  
11 Poulson, X. Wang, B. Xing and Y. Yang, Microbial transformation of multiwalled carbon  
12 nanotubes by *Mycobacterium vanbaalenii* PYR-1, *Environ. Sci. Technol.*, 2017, **51**, 2068–  
13 2076.  
14  
15 27. Y. Ge, J. H. Priester, M. Mortimer, C. H. Chang, Z. Ji, J. P. Schimel and P. A. Holden, Long-  
16 term effects of multiwalled carbon nanotubes and graphene on microbial communities in dry  
17 soil, *Environ. Sci. Technol.*, 2016, **50**, 3965–3974.  
18  
19 28. Y. Ge, C. Shen, Y. Wang, Y.-Q. Sun, J. P. Schimel, J. L. Gardea-Torresdey and P. A.  
20 Holden, Carbonaceous nanomaterials have higher effects on soybean rhizosphere prokaryotic  
21 communities during the reproductive growth phase than during vegetative growth, *Environ.*  
22 *Sci. Technol.*, 2018, **52**, 6636–6646.  
23  
24 29. F. Zhao, X. Xin, Y. Cao, D. Su, P. Ji, Z. Zhu and Z. He, Use of carbon nanoparticles to  
25 improve soil fertility, crop growth and nutrient uptake by corn (*Zea mays* L.), *Nanomaterials*,  
26 2021, **11**, 2717.  
27  
28 30. F. Gottschalk, T. Sun and B. Nowack, Environmental concentrations of engineered  
29 nanomaterials: review of modeling and analytical studies, *Environ. Pollut.*, 2013, **181**, 287–  
30 300.  
31  
32 31. A. A. Keller and A. Lazareva, Predicted releases of engineered nanomaterials: From global  
33 to regional to local, *Environ. Sci. Technol. Lett.*, 2013, **1**, 65–70.  
34  
35 32. M. R. McPherson, P. Wang, E. L. Marsh, R. B. Mitchell and D. P. Schachtman, Isolation and  
36 analysis of microbial communities in soil, rhizosphere, and roots in perennial grass  
37 experiments, *J. Vis. Exp.*, 2018, **137**, 57932.  
38  
39 33. T. Simmons, D. F. Caddell, S. Deng and D. Coleman-Derr, Exploring the root microbiome:  
40 extracting bacterial community data from the soil, rhizosphere, and root endosphere, *J. Vis.*  
41 *Exp.*, 2018, **135**, 57561.  
42  
43 34. A. Gryta, M. Frąc and K. Oszust, The application of the Biolog EcoPlate approach in  
44 ecotoxicological evaluation of dairy sewage sludge, *Appl. Biochem. Biotechnol.*, 2014, **174**,  
45 1434–1443.  
46  
47 35. M. R. Green and J. Sambrook, Precipitation of DNA with ethanol, *Cold Spring Harb. Protoc.*,  
48 2016, **12**, pdb.prot093377.  
49  
50  
51  
52  
53  
54  
55  
56  
57  
58  
59  
60

- 1  
2  
3 36. Y. You, K. Aho, K. A. Lohse, S. G. Schwabedissen, R. N. Ledbetter and T. S. Magnuson,  
4 Biological soil crust bacterial communities vary along climatic and shrub cover gradients within  
5 a sagebrush steppe ecosystem, *Front. Microbiol.*, 2021, **12**, 1096.  
6  
7 37. C. Marotz, A. Sharma, G. Humphrey, N. Gottel, C. Daum, J. A. Gilbert, E. Eloë-Fadrosh and  
8 R. Knight, Triplicate PCR reactions for 16S rRNA gene amplicon sequencing are unnecessary,  
9 *BioTechniques*, 2019, **67**, 29–32.  
10  
11 38. J. G. Caporaso, C. L. Lauber, W. A. Walters, D. Berg-Lyons, J. Huntley, N. Fierer, S. M.  
12 Owens, J. Betley, L. Fraser, M. Bauer, N. Gormley, J. A. Gilbert, G. Smith and R. Knight, Ultra-  
13 high-throughput microbial community analysis on the Illumina HiSeq and MiSeq platforms, *The*  
14 *ISME J*, 2012, **6**, 1621–1624.  
15  
16 39. A. Apprill, S. McNally, R. Parsons and L. Weber, Minor revision to V4 region SSU rRNA  
17 806R gene primer greatly increases detection of SAR11 bacterioplankton, *Aquat. Microb.*  
18 *Ecol.*, 2015, **75**, 129–137.  
19  
20 40. A. E. Parada, D. M. Needham and J. A. Fuhrman, Every base matters: Assessing small  
21 subunit rRNA primers for marine microbiomes with mock communities, time series and global  
22 field samples, *Environ. Microbiol.*, 2016, **18**, 1403–1414.  
23  
24 41. W. Walters, E. R. Hyde, D. Berg-Lyons, G. Ackermann, G. Humphrey, A. Parada, J. A.  
25 Gilbert, J. K. Jansson, J. G. Caporaso, J. A. Fuhrman, A. Apprill and R. Knight, Improved  
26 bacterial 16S rRNA gene (V4 and V4-5) and fungal internal transcribed spacer marker gene  
27 primers for microbial community surveys, *mSystems*, 2016, **1**, e00009-15.  
28  
29 42. S. Andrews, 2010. FastQC: a quality control tool for high throughput sequence data,  
30 <http://www.bioinformatics.babraham.ac.uk/projects/fastqc>.  
31  
32 43. E. Bolyen, J. R. Rideout, M. R. Dillon, N. A. Bokulich, C. C. Abnet, G. A. Al-Ghalith, H.  
33 Alexander, E. J. Alm, M. Arumugam, F. Asnicar, Y. Bai, J. E. Bisanz, K. Bittinger, A. Brejnrod,  
34 C. J. Brislawn, C. T. Brown, B. J. Callahan, A. x000E9 s M. C.-R. x000ED guez, J. Chase, E.  
35 K. Cope, R. Silva, C. Diener, P. C. Dorrestein, G. M. Douglas, D. M. Durall, C. Duvallet, C. F.  
36 Edwardson, M. Ernst, M. Estaki, J. Fouquier, J. M. Gauglitz, S. M. Gibbons, D. L. Gibson, A.  
37 Gonzalez, K. Gorlick, J. Guo, B. Hillmann, S. Holmes, H. Holste, C. Huttenhower, G. A.  
38 Huttley, S. Janssen, A. K. Jarmusch, L. Jiang, B. D. Kaehler, K. Bin Kang, C. R. Keefe, P.  
39 Keim, S. T. Kelley, D. Knights, I. Koester, T. Kosciulek, J. Kreps, M. G. I. Langille, J. Lee, R.  
40 Ley, Y.-X. Liu, E. Lottfield, C. Lozupone, M. Maher, C. Marotz, B. D. Martin, D. McDonald, L. J.  
41 McIver, A. V. Melnik, J. L. Metcalf, S. C. Morgan, J. T. Morton, A. T. Naimey, J. A. Navas-  
42 Molina, L. F. Nothias, S. B. Orchanian, T. Pearson, S. L. Peoples, D. Petras, M. L. Preuss, E.  
43 Pruesse, L. B. Rasmussen, A. Rivers, M. S. Robeson, P. Rosenthal, N. Segata, M. Shaffer, A.  
44 Shiffer, R. Sinha, S. J. Song, J. R. Spear, A. D. Swafford, L. R. Thompson, P. J. Torres, P.  
45 Trinh, A. Tripathi, P. J. Turnbaugh, S. Ul-Hasan, J. J. J. Hooft, F. Vargas, Y. V. x000E1 zquez-  
46 Baeza, E. Vogtmann, M. von Hippel, W. Walters, Y. Wan, M. Wang, J. Warren, K. C. Weber,  
47 C. H. D. Williamson, A. D. Willis, Z. Z. Xu, J. R. Zaneveld, Y. Zhang, Q. Zhu, R. Knight and J.  
48 G. Caporaso, Reproducible, interactive, scalable and extensible microbiome data science  
49 using QIIME 2, *Nat. Biotechnol.*, 2019, **37**, 852-857.  
50  
51  
52  
53  
54  
55  
56  
57  
58  
59  
60

- 1  
2  
3 44. B. J. Callahan, P. J. McMurdie, M. J. Rosen, A. W. Han, A. J. A. Johnson and S. P. Holmes,  
4 DADA2: high-resolution sample inference from Illumina amplicon data, *Nat. Methods*, 2016,  
5 **13**, 581–583.  
6  
7 45. B. J. Callahan, P. J. McMurdie and S. P. Holmes, Exact sequence variants should replace  
8 operational taxonomic units in marker-gene data analysis, *The ISME J*, 2017, **11**, 2639–2643.  
9  
10 46. C. Quast, E. Pruesse, P. Yilmaz, J. Gerken, T. Schweer, P. Yarza, J. Peplies and F. O.  
11 Glöckner, The SILVA ribosomal RNA gene database project: improved data processing and  
12 web-based tools, *Nucleic Acids Res.*, 2012, **41**, D590–D596.  
13  
14 47. N. A. Bokulich, B. D. Kaehler, J. R. Rideout, M. Dillon, E. Bolyen, R. Knight, G. A. Huttley  
15 and J. Gregory Caporaso, Optimizing taxonomic classification of marker-gene amplicon  
16 sequences with QIIME 2's q2-feature-classifier plugin, *Microbiome*, 2018, **6**, 90.  
17  
18 48. C. Lozupone and R. Knight, UniFrac: a new phylogenetic method for comparing microbial  
19 communities, *Appl. Environ. Microbiol.*, 2005, **71**, 8228–8235.  
20  
21 49. N. Segata, J. Izard, L. Waldron, D. Gevers, L. Miropolsky, W. S. Garrett and C.  
22 Huttenhower, Metagenomic biomarker discovery and explanation, *Genome Biol.*, 2011, **12**,  
23 R60.  
24  
25 50. G. M. Douglas, V. J. Maffei, J. R. Zaneveld, S. N. Yurgel, J. R. Brown, C. M. Taylor, C.  
26 Huttenhower and M. G. I. Langille, PICRUSt2 for prediction of metagenome functions, *Nat.*  
27 *Biotechnol.*, 2020, **38**, 685–688.  
28  
29 51. M. I. Love, W. Huber and S. Anders, Moderated estimation of fold change and dispersion for  
30 RNA-seq data with DESeq2, *Genome Biol.*, 2014, **15**, 550.  
31  
32 52. J. Chong, P. Liu, G. Zhou and J. Xia, Using MicrobiomeAnalyst for comprehensive  
33 statistical, functional, and meta-analysis of microbiome data, *Nat. Protoc.*, 2020, **15**, 799–821.  
34  
35 53. R Core Team, 2013. R: A language and environment for statistical computing.  
36  
37 54. J. Oksanen, F. G. Blanchet, R. Kindt, P. Legendre, P. R. Minchin, R. B. O'hara, G. L.  
38 Simpson, P. Solymos, M. H. H. Stevens, H. Wagner and M. J. Oksanen, 2013. 'vegan',  
39 Community Ecology Package, version 2(9), 1-295.  
40  
41 55. P. J. McMurdie and S. Holmes, phyloseq: an R package for reproducible interactive analysis  
42 and graphics of microbiome census data, *PLoS ONE*, 2013, **8**, e61217-11.  
43  
44 56. H. Wickham, ggplot2, *WIREs Comp Stat*, 2011, **3**, 180–185.  
45  
46 57. H. Wickham, M. Averick, J. Bryan, W. Chang, L. McGowan, R. François, G. Golemund, A.  
47 Hayes, L. Henry, J. Hester, M. Kuhn, T. Pedersen, E. Miller, S. Bache, K. Müller, J. Ooms, D.  
48 Robinson, D. Seidel, V. Spinu, K. Takahashi, D. Vaughan, C. Wilke, K. Woo and H. Yutani,  
49 Welcome to the Tidyverse, *JOSS*, 2019, **4**, 1686.  
50  
51  
52  
53  
54  
55  
56  
57  
58  
59  
60

- 1  
2  
3 58. P. L. Buttigieg and A. Ramette, A guide to statistical analysis in microbial ecology: a  
4 community-focused, living review of multivariate data analyses, *FEMS Microbiol. Ecol.*, 2014,  
5 **90**, 543–550.  
6  
7 59. M. J. Anderson, A new method for non-parametric multivariate analysis of variance, *Austral.*  
8 *Ecol.*, 2001, **26**, 32–46.  
9  
10 60. B. J. Callahan, K. Sankaran, J. A. Fukuyama, P. J. McMurdie and S. P. Holmes,  
11 Bioconductor workflow for microbiome data analysis: from raw reads to community analyses,  
12 *F1000Res*, 2016, **5**, 1492–49.  
13  
14 61. Y. Wang, C. H. Chang, Z. Ji, D. C. Bouchard, R. M. Nisbet, J. P. Schimel, J. L. Gardea-  
15 Torresdey and P. A. Holden, Agglomeration determines effects of carbonaceous  
16 nanomaterials on soybean nodulation, dinitrogen fixation potential, and growth in soil, *ACS*  
17 *Nano*, 2017, **11**, 5753–5765.  
18  
19 62. R. Baby, B. Saifullah and M. Z. Hussein, Carbon nanomaterials for the treatment of heavy  
20 metal-contaminated water and environmental remediation, *Nanoscale Res. Lett.*, 2019, **14**,  
21 341.  
22  
23 63. P. Zhang, Z. Guo, Z. Zhang, H. Fu, J. C. White and I. Lynch, Nanomaterial transformation in  
24 the soil–plant system: Implications for food safety and application in agriculture, *Small*, 2020,  
25 **16**, 2000705.  
26  
27 64. M. V. Langwig, V. De Anda, N. Dombrowski, K. W. Seitz, I. M. Rambo, C. Greening, A. P.  
28 Teske and B. J. Baker, Large-scale protein level comparison of Deltaproteobacteria reveals  
29 cohesive metabolic groups, *The ISME J*, 2022, **16**, 307–320.  
30  
31 65. Y. Zhu, Q. Li, D. Kim, Y. Min, B. Lee and Y. S. Jun, Sulfate-controlled heterogeneous  
32 CaCO<sub>3</sub> nucleation and its non-linear interfacial energy evolution, *Environ. Sci. Technol.*, 2021,  
33 **55**, 11455–11464.  
34  
35 66. A. M. Kielak, C. C. Barreto, G. A. Kowalchuk, J. A. van Veen and E. E. Kuramae, The  
36 ecology of *Acidobacteria*: moving beyond genes and genomes, *Front. Microbiol.*, 2016, **7**, 744.  
37  
38 67. M. Mortimer, N. Devarajan, D. Li and P. A. Holden, Multiwall carbon nanotubes induce more  
39 pronounced transcriptomic responses in *Pseudomonas aeruginosa* PG201 than graphene,  
40 exfoliated boron nitride, or carbon black, *ACS Nano*, 2018, **12**, 2728–2740.  
41  
42 68. M. Mortimer, D. Li, Y. Wang and P. A. Holden, Physical properties of carbon nanomaterials  
43 and nanoceria affect pathways important to the nodulation competitiveness of the symbiotic  
44 N<sub>2</sub>-fixing bacterium *Bradyrhizobium diazoefficiens*, *Small*, 2020, **16**, 1906055.  
45  
46 69. V. I. Lushchak and N. M. Semchuk, Tocopherol biosynthesis: chemistry, regulation and  
47 effects of environmental factors, *Acta Physiol. Plant*, 2012, **34**, 1607–1628.  
48  
49 70. R. Grinter and C. Greening, Cofactor F420: an expanded view of its distribution,  
50 biosynthesis and roles in bacteria and archaea, *FEMS Microbiol. Rev.*, 2021, **45**, fuab021.  
51  
52  
53  
54  
55  
56  
57  
58  
59  
60

- 1  
2  
3 71. E. A. Davidson, I. A. Janssens and Y. Luo, On the variability of respiration in terrestrial  
4 ecosystems: moving beyond Q10, *Glob. Change Biol.*, 2006, **12**, 154–164.  
5  
6 72. M. Xu and H. Shang, Contribution of soil respiration to the global carbon equation, *J. Plant*  
7 *Physiol.*, 2016, **203**, 16–28.  
8  
9 73. V. Vives-Peris, C. de Ollas, A. Gómez-Cadenas and R. M. Pérez-Clemente, Root exudates:  
10 from plant to rhizosphere and beyond, *Plant Cell Rep.*, 2020, **39**, 3–17.  
11  
12  
13  
14  
15  
16  
17  
18  
19  
20  
21  
22  
23  
24  
25  
26  
27  
28  
29  
30  
31  
32  
33  
34  
35  
36  
37  
38  
39  
40  
41  
42  
43  
44  
45  
46  
47  
48  
49  
50  
51  
52  
53  
54  
55  
56  
57  
58  
59  
60

**Figure 1.** Venn diagram showing ASVs identified in the soils receiving different treatments.

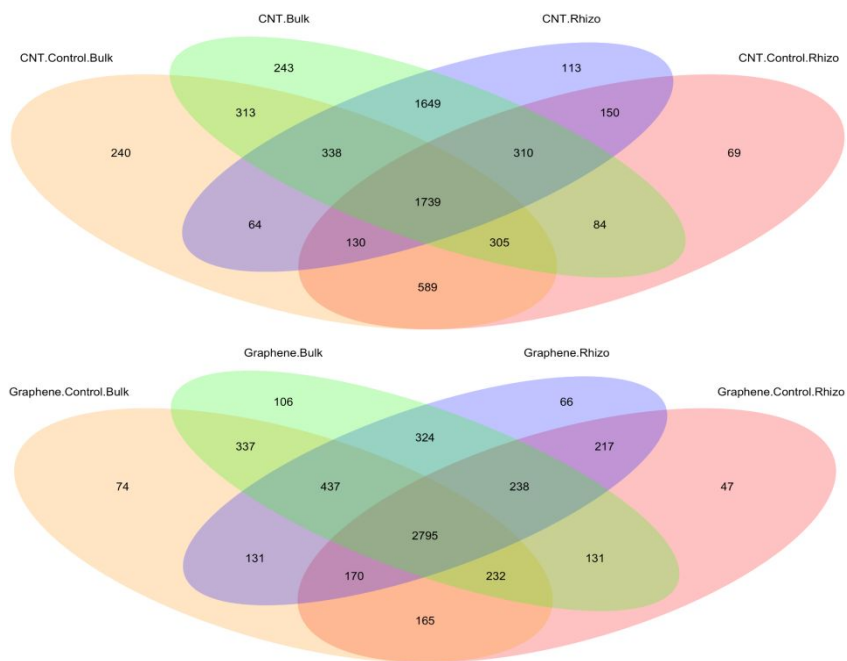


**Figure 2.** Effects of CNT (left) and graphene (right) on microbial Shannon diversity in bulk soil and the tomato rhizosphere.

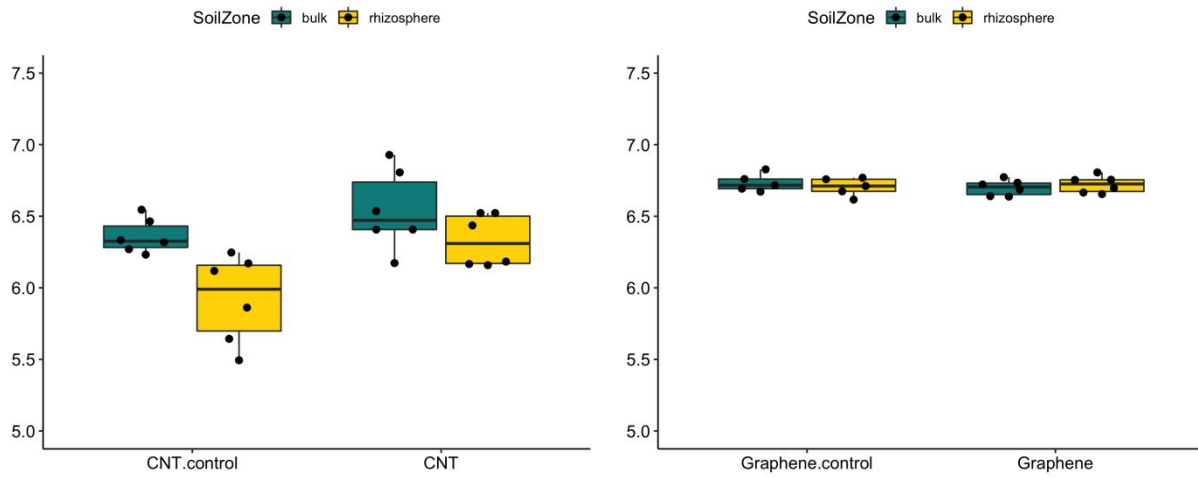


**Figure 3.** Effects of CNT (upper) and graphene (lower) on microbial beta diversity in bulk soil and the tomato rhizosphere. PCoA was based on Bray-Curtis distance of log-transformed ASV abundance. Ellipses are 95% confidence intervals for each treatment.

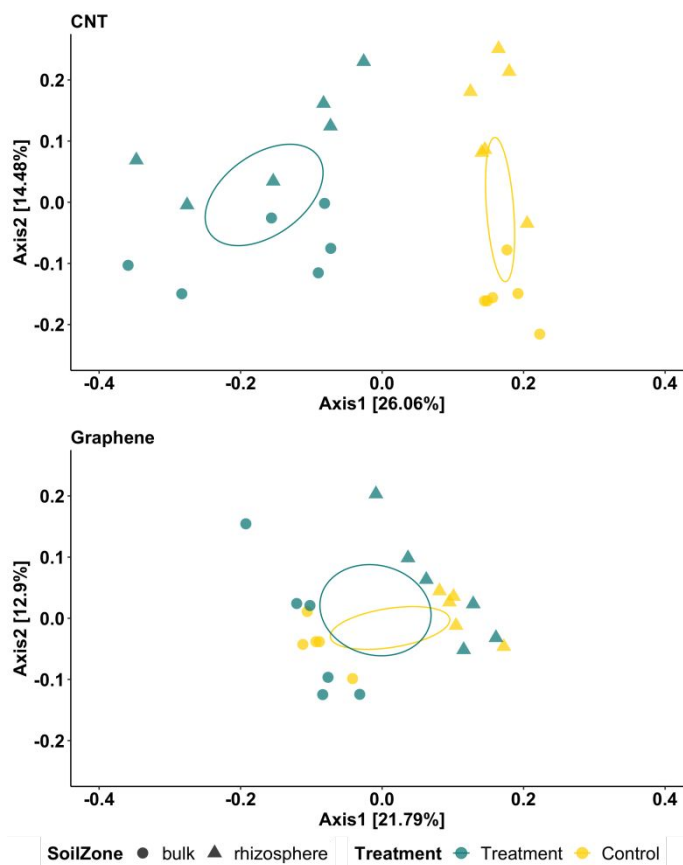


**Figure 4.** Effects of CNT (left) and graphene (right) on the relative abundance of the top 10 phyla in bulk soil and the tomato rhizosphere. Data present averages across biological replicates.

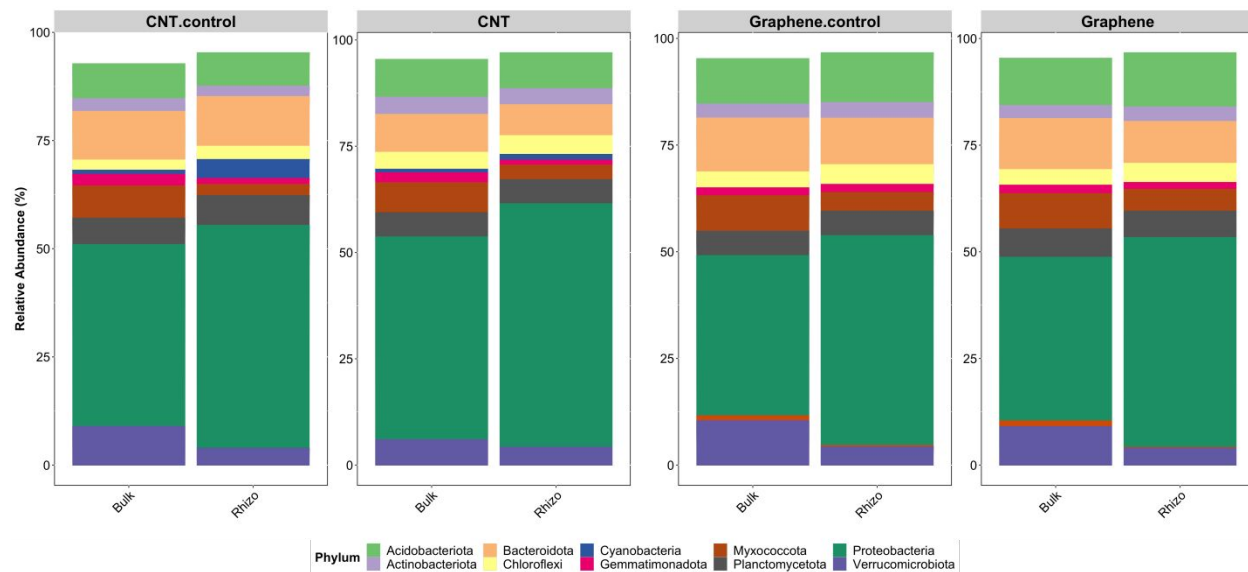


**Figure 5.** CNT influenced more microbial taxa in bulk soil (upper left) than the tomato rhizosphere (upper right). Graphene treatment influenced less microbial taxa in bulk soil (lower left) than the tomato rhizosphere (lower right). Only phyla and classes are shown here.

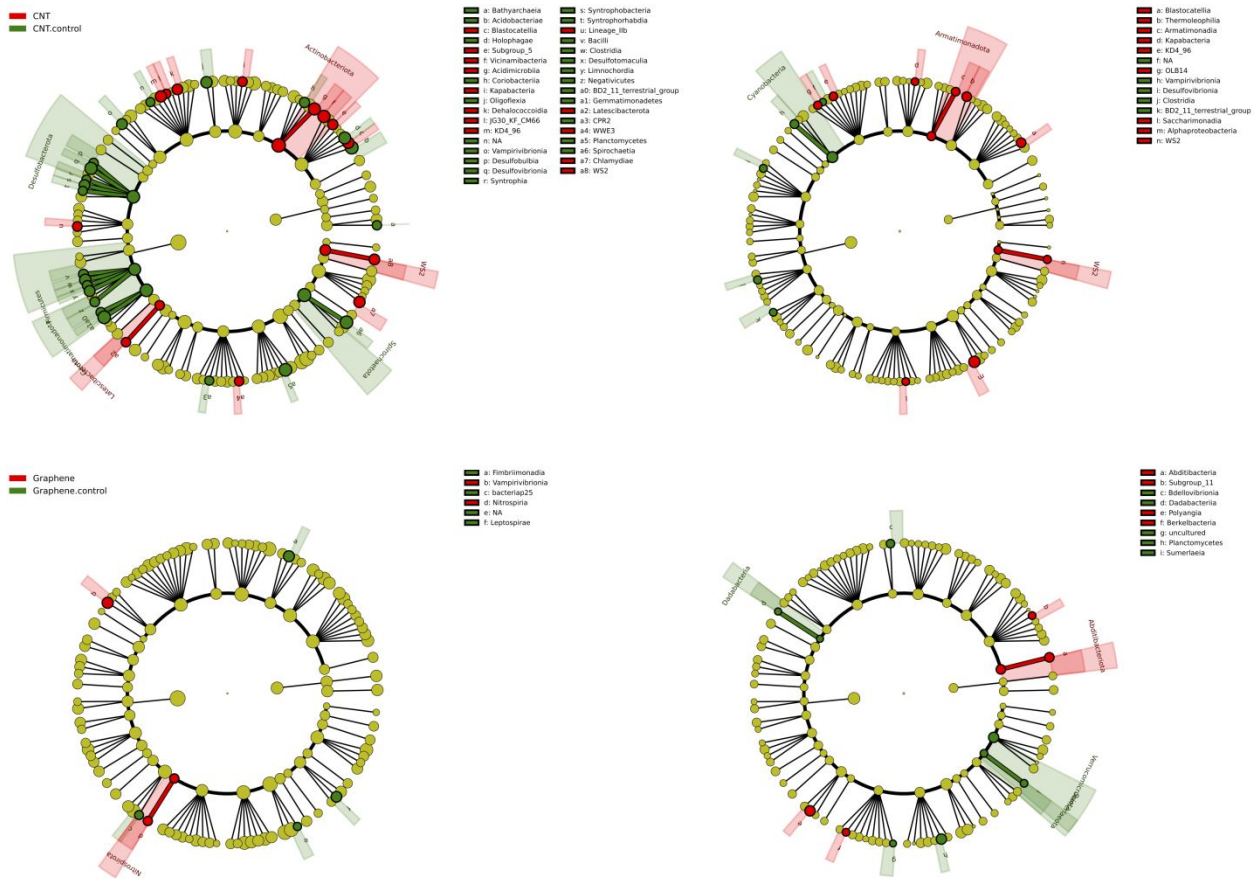


**Figure 6.** Effects of CNT and graphene on the phylum-level microbial network in the tomato rhizosphere. Networks were calculated based on Bray-Curtis distance with a maximum distance of 0.3.

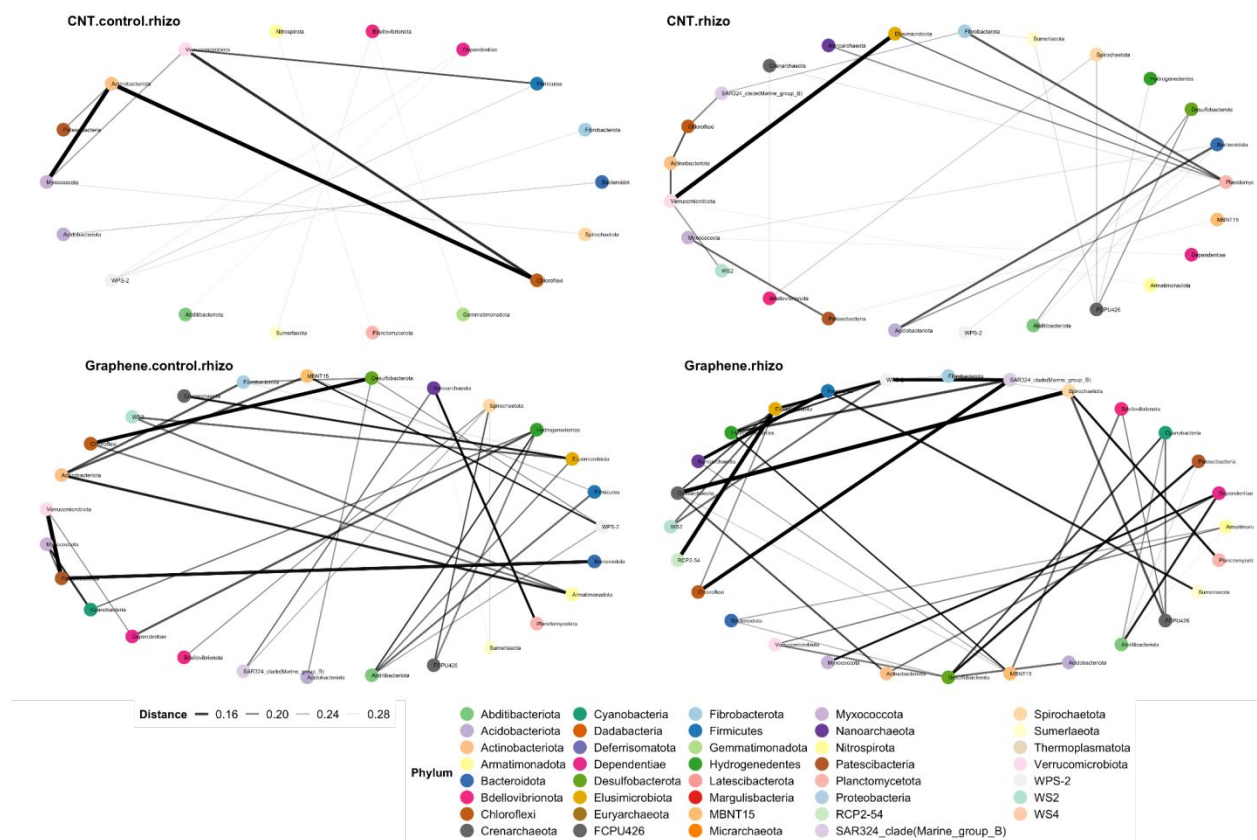


**Figure 7.** Heatmap showing CNT and graphene effects on microbial substrate utilization. AWCD values were averaged across technique replicates and pot replicates and normalized against corresponding controls. The color key indicates fold change. Asterisks and number signs indicate substrate compound significantly affected by CNT or graphene, respectively, as compared to controls ( $p < 0.05$  in Kruskal-Wallis test). Substrate categories are presented on the right side of the heatmap with substrate complexity increasing from bottom to top as annotated by the grey arrow.

